Advanced Ion Beam Calorimetry for the Test Facility ELISE

R. Nocentini[1, a)], F. Bonomo[2,3], A. Pimazzoni[4], U. Fantz[1], P. Franzen[1], M. Fröschle[1], B. Heinemann[1], R. Pasqualotto[2], R. Riedl[1], B. Ruf[1], D. Wünderlich[1]

[1] *Max-Planck-Institut für Plasmaphysik, Boltzmannstr. 2, 85748 Garching, Germany*
[2] *Consorzio RFX(CNR, ENEA, INFN, Università di Padova, Acciaierie Venete SpA), Corso Stati Uniti 4, 35127 Padova, Italy*
[3] *Istituto Gas Ionizzati - CNR, Corso Stati Uniti 4, 35127 Padova, Italy*
[4] *Università degli Studi di Padova, Via 8 Febbraio 2, 35122 Padova, Italy*

[a)]Corresponding author: riccardo.nocentini@ipp.mpg.de

Abstract. The negative ion source test facility ELISE (Extraction from a Large Ion Source Experiment) is in operation since beginning of 2013 at the Max-Planck-Institut für Plasmaphysik (IPP) in Garching bei München. The large radio frequency driven ion source of ELISE is about 1x1 m^2 in size (1/2 the ITER source) and can produce a plasma for up to 1 h. Negative ions can be extracted and accelerated by an ITER-like extraction system made of 3 grids with an area of 0.1 m^2, for 10 s every 3 minutes. A total accelerating voltage of up to 60 kV is available, i.e. a maximum ion beam power of about 1.2 MW can be produced. ELISE is equipped with several beam diagnostic tools for the evaluation of the beam characteristics. In order to evaluate the beam properties with a high level of detail, a sophisticated diagnostic calorimeter has been installed in the test facility at the end of 2013, starting operation in January 2014. The diagnostic calorimeter is split into 4 copper plates with separate water calorimetry for each of the plates. Each calorimeter plate is made of 15x15 copper blocks, which act as many separate inertial calorimeters and are attached to a copper plate with an embedded cooling circuit. The block geometry and the connection with the cooling plate are optimized to accurately measure the time-averaged power of the 10 s ion beam. The surface of the blocks is covered with a black coating that allows infrared (IR) thermography which provides a 2D profile of the beam power density. In order to calibrate the IR thermography, 48 thermocouples are installed in as many blocks, arranged in two vertical and two horizontal rows. The paper describes the beam calorimetry in ELISE, including the methods used for the IR thermography, the water calorimetry and the analytical methods for beam profile evaluation. It is shown how the maximum beam inhomogeneity amounts to 13% in average. The beam divergence derived by IR thermography ranges between 1° and 4° and correlates relatively well with the values measured by beam emission spectroscopy with up to 30% difference. It has also been observed that the beam inhomogeneity decreases with lower beam divergence.

INTRODUCTION

In order to provide additional heating power and current drive for the international nuclear fusion experiment ITER presently under construction in Cadarache (France), a new neutral beam injection system is being developed [1]. In ITER, two neutral beam injectors will provide about 17 MW of heating power each by means of injection of neutral particles which are accelerated up to 1 MeV. The negative ion source for the production and acceleration of such particles is based on the IPP prototype RF sources [3]-[7]. These negative ion sources, developed in the past decades, have achieved all the ITER requirements, but not simultaneously and with a source size smaller (extraction areas up to 200 cm^2) than the source necessary for ITER (extraction area of 2000 cm^2). The test bed ELISE (Extraction from a Large Ion Source Experiment) [8]-[10] has been developed at IPP as an intermediate step

between the small prototype sources and the ITER-size negative ion source. The ITER European domestic agency Fusion for Energy (F4E) has introduced the development of the RF ion source and of the extraction system into the R&D roadmap for the ITER NBI system in order to demonstrate the necessary plasma and beam uniformity and ELISE is an important step in this roadmap.

ELISE is designed to achieve ITER-relevant parameters [11] simultaneously using the largest RF negative ion source built so far (extraction grid surface of about 1 x 1 m^2) which is half of the ITER source. ELISE is operated using H or D and is designed to produce plasma continuously for up to 1 h. By means of a three-grid extraction system, a negative ion beam can be extracted and accelerated up to 60 kV for 10 s every 3 minutes, due to limits of the IPP high-voltage power supplies. The ITER-like extraction system is made of 640 beamlets, arranged in 2 rows of 4 beamlet groups each [12].

A magnetic filter field of up to 5 mT can be produced in ELISE by means of a strong electric current of up to 5.3 kA flowing through the first grid and return conductors [13].

ELISE started operation in the beginning of 2013. Power from the two RF generators (feeding two drivers each) as well as plasma pulse duration have since then been gradually increased, starting from 40 kW up to 110 kW per generator and reaching several minutes of continuous plasma operation. RF pulses in both H and D with beam extraction have been performed and the current results have been summarized in [10].

ELISE is equipped with several diagnostic tools in order to evaluate plasma [14] and beam [15] properties. This paper focuses on the latest developments on the calorimetric beam diagnostic tools. In order to reconstruct a 2D map of the beam power distribution and obtain information about the beam divergence and inhomogeneity, a sophisticated copper diagnostic calorimeter has been designed and manufactured in the last years and finally installed in ELISE at the beginning of 2014. Its front side (beam target surface) has been covered with a blackening spray in order to increase its emission coefficient. An infrared (IR) camera looking at the calorimeter allows to measure the bi-dimensional temperature distribution on its surface and to evaluate the beam power distribution with a resolution of 30 x 30 "pixels".

THE BEAM DIAGNOSTIC CALORIMETER

The diagnostic calorimeter is made of 4 copper plates, as shown in FIGURE 1(a), each one having a size of about 600 mm x 600 mm, resulting in a total calorimeter dimension of about 1.2 m x 1.2 m, and with a thickness of 41 mm. The calorimeter plates are installed inside the ELISE vacuum tank at about 3.5 m from the grounded grid and are attached to a piping structure that provides water inlets and outlets for the cooling circuits of each plate and at the same time supports the copper plates. The cooling circuit has separated water outlets in order to allow individual water calorimetry for each plate and therefore a beam power measurement for each one of the four calorimeter "sectors". In addition, 12 thermocouples (TCs) have been embedded in each plate, in the positions shown in FIGURE 1(c), in order to calibrate the IR thermography, as described below, and to perform beam profile measurements over two vertical and two horizontal lines.

The diagnostic calorimeter has been designed to be operated inertially, i.e. the heat is stored in the copper mass during the beam pulse and is removed in between the beam pulse, allowing easy power evaluation.

Each calorimeter plate is made of a cooling back plate, with an embedded cooling circuit, and 15 x 15 copper blocks which are brazed to the "beam side" of the calorimeter. Each block is inertially cooled via small cooling channels in the back plate and through a small ø10 mm x 2 mm copper cylinder that acts as a thermal resistance between cooling plate and block. In this way, the heat transfer between block and cooling plate is small and well defined, allowing for a precise measurement of the power deposited during the beam pulse [15]. Each block has a surface of 38 mm x 38 mm and a thickness of 25 mm. The block thickness of 25 mm has been chosen to allow a maximum temperature of 450°C for an expected maximum power density of 3 MW/m^2 (1.2 MW total beam power, 2° divergent beam). The embedded thermocouples are positioned at half depth of a block in order to provide a good estimate of the average block temperature. Each block is separated from adjacent blocks by a 2 mm gap. With this solution the transversal heat transmission between blocks during the beam phase is practically negligible.

This design allows a beam power estimate from the mean block temperature with an error below 5%. Even if the calorimeter is hit by a beam with maximum power (1.2 MW), it is still possible to lower the block temperature to about 40°C after a 3 min. pause, before the next beam pulse.

The heavy cooling in the back plate and the fact that it is covered by the blocks, make its maximum temperature relatively low (~100°C). This fact, together with the separation of the blocks, reduces the thermo-mechanical stress and deformation in the calorimeter plates.

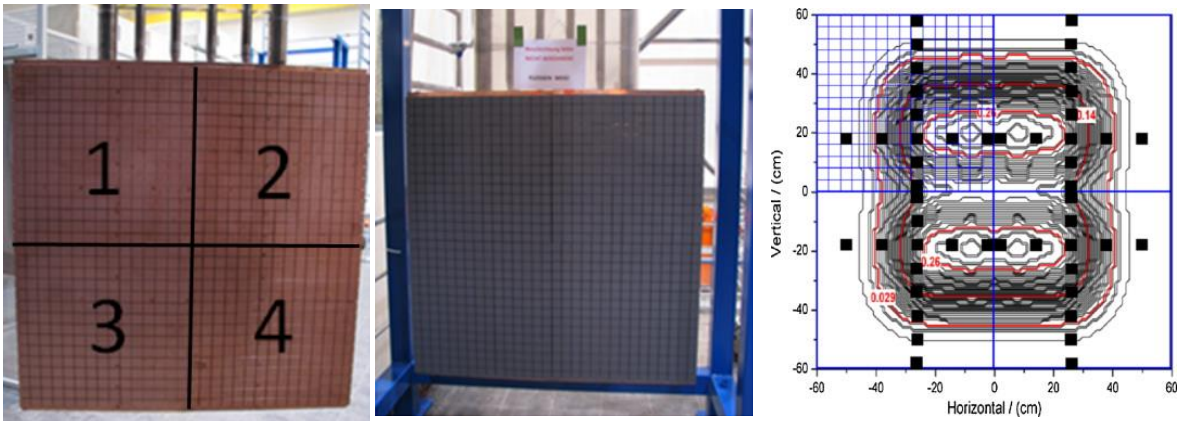

(a) (b) (c)

FIGURE 1. The diagnostic calorimeter of ELISE before (a) (the four sectors are indicated) and after (b) the target surface blackening. In (c) the positions of the 48 thermocouples are shown, together with the calculated deposited power distribution for a beam of 1.2 MW total power and 2° divergence (values in kW/cm^2).

The diagnostic calorimeter is observed by an IR camera, with the aim to measure the average temperatures of each block and therefore obtain a 2D image of the beam power distribution, with a resolution of 30 x 30 "pixels". In order to reduce the reflectivity of the copper surface, the target surface of the blocks has been covered by means of a MoS_2 spray coating with a high IR emissivity coefficient; see FIGURE 1(b). The MoS_2 spray coating has been favored among other solutions, which have been extensively tested using a temporary beam dump installed in ELISE during 2013. The MoS_2 spray coating is easy to apply and has very low cost, which are important factors considering the uncertainty on durability and constancy of the emissivity coefficient of IR black coatings under energetic negative hydrogen ion bombardment.

The measurement of the emissivity coefficient of the IR black coating is fundamental for the calibration of the IR diagnostic and this has been performed using the signal from the thermocouples installed in the diagnostic calorimeter.

IR MEASUREMENTS

In order to evaluate the beam power deposition on the diagnostic calorimeter, a FLIR A655sc IR micro-bolometer camera is currently being used in the ELISE testbed. This camera has a spectral range of 7.8-14 μm, and a resolution of 640 (h) x 480 (v) pixels. The camera is installed on one of the lateral ports of the vacuum tank of ELISE, looking at the calorimeter with a wide angle objective that provides a 45°(v) x 34°(h) field of view. An example of the IR image during a beam pulse is shown in FIGURE 2. The beam heats up the central part of the calorimeter: the beamlet divergence for this example is small enough to allow to distinguish the upper and lower beam segments and also the four central beamlet groups. The beam deflection due to the magnetic filter field is also visible. The calorimeter view is limited by the round porthole, as visible in FIGURE 2. The more external blocks are affected by some vignetting and they

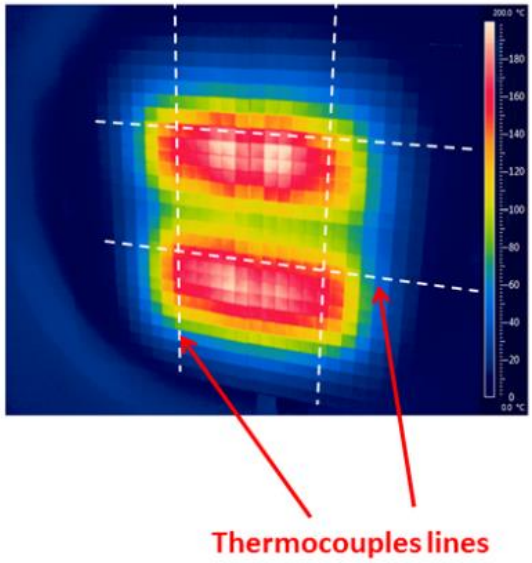

FIGURE 2. IR image of a beam in ELISE. With the upper and lower beam segment, also the four central beamlet groups can be clearly distinguished. Pulse #6188, Hydrogen, RF power of 2x81 kW, U_{HV} = 35.5 kV, I_{PG} = 2 kA, I_{bias} = 55 A, j_{extr} = 16.47 mA/cm^2, j_e/j_{extr} = 0.4. The dashed lines represent the beam profiles that can be measured by means of the embedded thermocouples

are excluded by the beam power calculation (their contribution to the total beam power is negligible as they are not hit by the beam).

Since each calorimeter block is inertially cooled, the power deposited on it during the beam-on phase is approximately proportional to the temperature increase of the block. The IR camera measures the temperature of the blackened surface of the block, which is slightly higher (depending on the beam power) than the block bulk temperature. In order to obtain a measurement that is closer to the average temperature of the block, it is necessary to wait 1.5 s after the beam-off (see FIGURE 3). During this time, the temperature redistributes into the block and is more uniform. The temperature increase (ΔT) due to the single beam pulse is therefore obtained as the difference between the temperatures obtained at 1.5 s after the beam is off and the one just before the beam-on phase. The power deposition is then calculated simply by multiplying the ΔT times the heat capacity of a copper block and the beam-on time. Since there could be local non-uniformities of the black coating, the result from the IR temperature measurement is averaged over the surface of a block. The pixels close to the block edges are not taken into consideration.

IR Data Calibration by Means of Thermocouples

The IR camera has been calibrated in order to obtain an accurate ΔT measurement for the beam power estimation. Several parameters have to be defined for the temperature calculation performed via the IR camera software. Most of these parameters come from the environment in which the measurement is done, like the temperature of reflected surfaces; others refer to the surface to be observed. Among the latters, the most critical parameters are the emissivity coefficients of the black surfaces. A too low emissivity coefficient means an over-estimation of the measured temperature, while the contrary happens for a too high emissivity coefficient. For this reason, an absolute calibration of the IR thermography been performed by comparing the temperature values measured in the 48 calorimeter blocks with TCs and the values obtained from the IR camera. The basic idea for this calculation is that in an inertial system the temperature increase due to a single beam pulse and the temperature evolution during the cool-down phase in the following beam-off phase should be the same both for TCs and the IR data. For each block housing a TC the temperature measured by the IR camera has been matched to the corresponding value measured by the TC during the cooling phase by finding the emissivity coefficient. It must be taken into account that during the beam-on phase the thin black surface coating of a block is heated up to a considerably higher temperature with respect to the block bulk material, as shown in FIGURE 3. This is mainly due to the contact resistance between coating and copper substrate and is highest during beam pulse. The temperature difference between block surface coating and copper substrate decreases quickly after the beam is switched off and is negligible during the cool-down phase in between two beam pulses.

The 48 emissivity coefficients for the corresponding blocks have therefore been calculated. In order to extend the IR temperature measurement to all the 900 blocks in the diagnostic calorimeter, an average value of the 48 emissivity coefficients has been used. This procedure has been performed for the first beam pulse of the day (to avoid the small error induced by a previous beam pulse) during several operation days between January and June 2014. During this time, the estimated emissivity coefficient has slightly decreased, as shown in FIGURE 4 (a). The emissivity coefficient shows a decrease in time, suggesting a possible degradation of the coating properties due to the beam operation. We can expect that the coating of the central calorimeter blocks, which are more heavily bombarded by the beam with respect to the peripheral ones, will show a higher degradation and consequent reduction of the emissivity coefficient with respect to the coating on the other blocks. The spatial distribution of the evaluated emissivities (as an average in time for each block) is shown in FIGURE 4(b); the shaded areas correspond

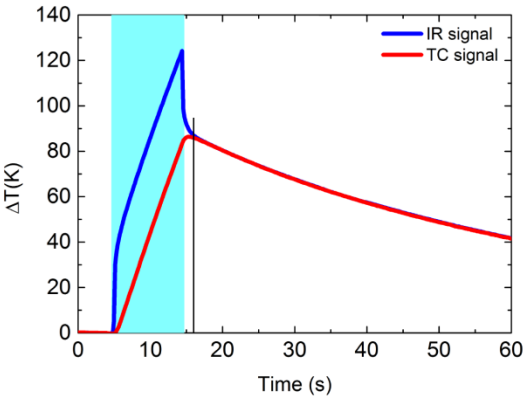

FIGURE 3. Comparison between TC and IR temperature signals for a block before, during and after a beam pulse. The shaded region represents the beam-on phase. Here the IR signal is shifted upwards with respect to the TC signal, due to the contact resistance between IR black coating and copper substrate. A proper emissivity coefficient has been calculated in order to match the two curves during the cool-down phase, starting from 1.5 seconds after beam-off, indicated by the black line.

to the incident position of beamlet groups, taking into account the deflection due to the magnetic filter field, where ion bombardment from the beam is higher. Inside these shaded areas, the emissivity coefficient is clearly lower than outside of them, indicating that, as expected, the black coating degradation is higher in the central region of the calorimeter, which is hit by the beam, than in the external blocks. Even though a spatial pattern in the calculated emissivity coefficient exists, an average coefficient value, constant in space and time, $\varepsilon = 0.83$, has been assumed to simplify the subsequent evaluation of beam divergence and inhomogeneity. This coefficient of emissivity has been assumed to be the same for all the blocks, and it is the value used for the investigation reported in this paper.

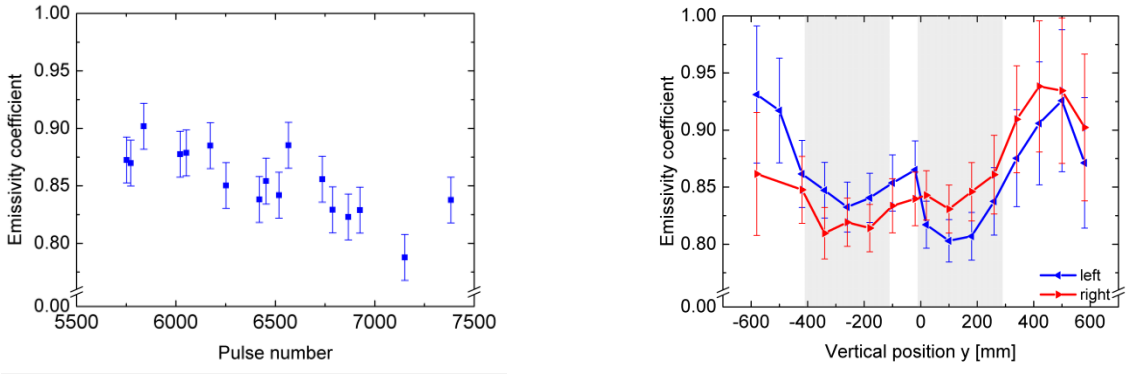

(a) (b)

FIGURE 4. (a) Evolution of emissivity coefficient for a central calorimeter block over time. The error, around 2 %, is calculated from a single measurement. (b) Distribution of emissivity coefficient along the vertical TC profiles. The shaded area corresponds to the vertical position of the beamlet groups, slightly bent down by the influence of the magnetic filter field.

BEAM POWER DEPOSITION ON THE CALORIMETER

For total power beam evaluation, two different calorimetric measurements have been performed in ELISE. The first one is based on water calorimetry by using the temperature measurement on the cooling water of the calorimeter back plates (four measurements, one for each panel); the second one is based on the IR measurement already introduced in the previous paragraph. Since the heat deposited on the block surface is transferred, mainly during the beam-off phase, to the back side of the calorimeter plate where it is removed by the cooling system, the two estimates should provide comparable values. Due to the 2 mm gaps between the blocks, the total power collected by the blocks and measured by IR thermography is slightly lower than what is measured from the water calorimetry. The temperature increase of the blocks as measured by the IR camera is due to the portion of the beam which directly hits the block target surface, while the power which is deposited in the 2 mm gaps between the blocks only slightly contributes to the increase of the block temperature. This portion of beam power hits the back plate and is removed by the water cooling. The ratio between the total target surface of the blocks and the total calorimeter size (i.e. the total the size of the four plates) is 0.9. The ratio between the two estimated power values is therefore expected (within measurements uncertainties) to be between 0.9 and 1, depending on the beam divergence.

A comparison between water calorimetry and IR calorimetry is performed by calculating the total current densities impinging on each calorimeter panel. The current densities are proportional to the deposited power, under the assumption that all the power is carried by particles at full energy, as $P = I \cdot U_{HV} = j \cdot A \cdot U_{HV}$, where P is the total beam power, I is the total ion current, U_{HV} is the total voltage, A the total area of the plasma grid apertures and j the negative ion current density. Since it is not straightforward to determine from which part of the grids the particles impinging on each panel come from (also in presence of a plasma vertical deflection due to the magnetic filter field), the area A used for calculation is the total extraction area (985 cm^2).

The correlation of the accelerated beam current densities impinging on each panel of the diagnostic calorimeter, calculated by IR measurements and water calorimetry, is shown in FIGURE 5. The current density estimates are linearly well-correlated in all the panels. In three panels, the slope of the fitting data is really close to the expected values (between 0.9 and 1); only for panel 1 it is below 0.9. This difference might be due to a slightly different water flow rate distribution in the panels 1 and 3 that affects the water calorimeter estimation. The cooling system of the panels has been designed to provide equal water flow rate in the four water circuits, however it is possible that some

machining inaccuracy has produced differences in the cooling channels dimensions, which in turn causes about 10% higher water flow rate in plate 1 than in plate 3. At the moment this explanation cannot be verified, as only one global water flow measurement is available for the four calorimeter panels.

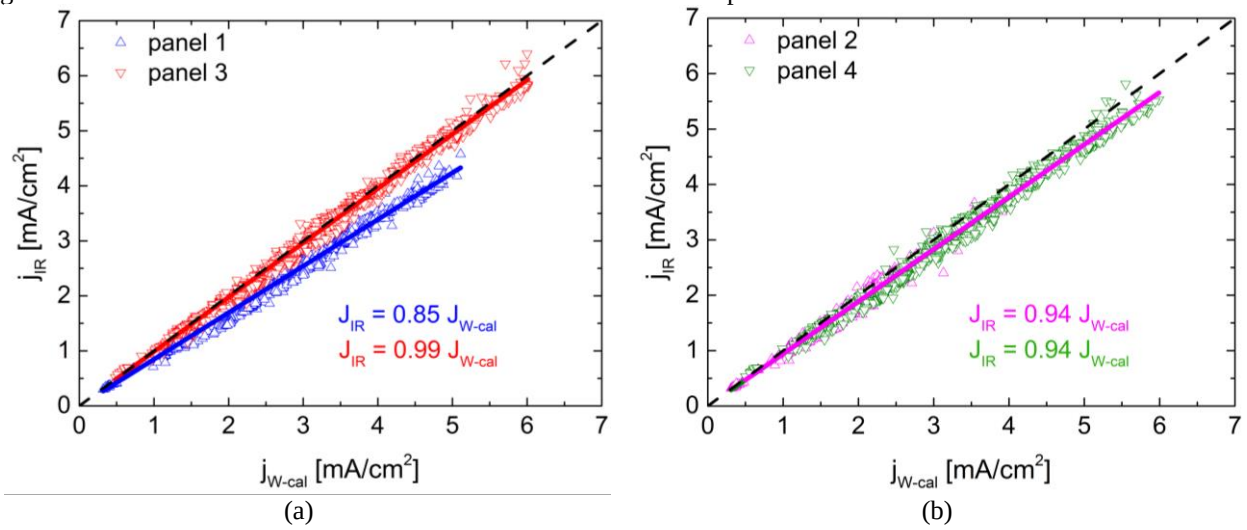

FIGURE 5. Current density on the four panels: IR thermography versus water calorimetry. Left: Panels 1 and 3. Right: Panels 2 and 4.

BEAM PROPERTIES CHARACTERIZATION

The information obtained from the measurement of the beam power distribution on the 30 x 30 blocks of the diagnostic calorimeter can be used to evaluate some beam properties. Among them, the most important ones are the beam divergence and the beam inhomogeneity. The divergence of the single beamlets cannot be derived directly from the IR image because the diagnostic calorimeter is positioned at 3.5 m downstream of the grounded grid. This means that for the typical divergences measured at ELISE (1° at minimum), the beamlets are largely overlapping. Nevertheless, the average divergence of the beamlets can be correlated to the divergence of beamlet groups.

The definition of beam inhomogeneity used for ITER refers to the deviation of single beamlet intensity with respect to the average beamlet intensity, but measuring such this kind of inhomogeneity is not possible at the moment, as sophisticated beam models are necessary and under development [16]. In ELISE the inhomogeneity is measured in terms of beam intensity of each beamlet group and the value of ion current (and so the power) of each beamlet group should not differ more than 10 % from the average of ion current (or powers) from all the beamlet groups.

In order to investigate the beamlet group properties, a fitting procedure has been developed: the power density profiles obtained by IR measurements are fitted by means of 8 gaussian "sub-beams", one for each beamlet group. The number of free parameters is kept as small as possible by assuming that the beamlet groups are partially associated: the vertical position of their centers is set to be equal for the four beamlet groups belonging to the same half grid (upper and lower segments); similarly, the width of the gaussian functions, both in the horizontal and in the vertical direction, are the same for the groups belonging to the same grid segment. In addition, the horizontal position of each beamlet group is assumed to correspond to the geometrical projection of the beamlet groups from the grounded grid onto the diagnostic calorimeter. In this way, the total number of free parameter is limited to 14: the 8 gaussian function amplitudes (one for each beamlet group), the four widths of the gaussians in the horizontal and vertical directions (σ_x^{top}, σ_x^{bottom} and σ_y^{top}, σ_y^{bottom}), and the vertical positions of the rows of beamlet groups (y^{top}, y^{bottom}). The widths of the beamlet groups can therefore be used to estimate the beamlet divergences, while the amplitudes can be used to estimate the beam inhomogeneity.

The sensitivity and reliability of the fitting procedure has been successfully tested, showing the capability of giving reliable information on the beamlet group amplitudes and widths for different beam shapes, even when the beamlet divergence is so large (> 2°) that the beam power profile corresponds to a unique bell-shaped function. Of course for very small divergences (< 1°) the gaussian function cannot reproduce accurately the rectangular shape of

a beamlet group.

An example of the 2D map of the power deposited on the calorimeter for a beam with a divergence of 1°, estimated by Beam Emission Spectroscopy (BES), is shown in FIGURE 6(a); the corresponding fit is displayed in FIGURE 6(b). The 2D power map reconstruction performed by the automatic fit is satisfactory: the residuals are for this example around 10% at maximum; at higher beam divergences, the residuals decrease below 5% for most of the cases.

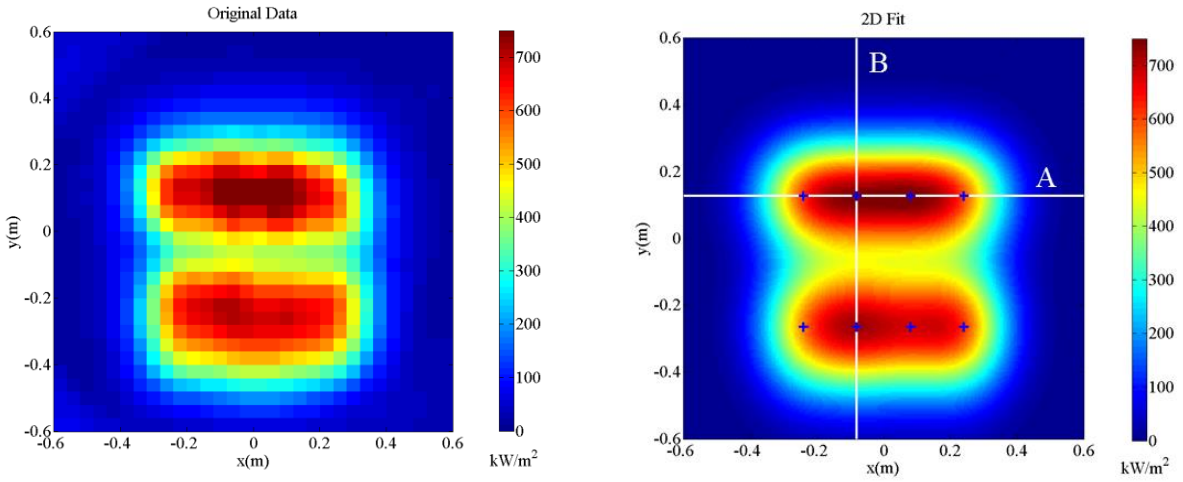

FIGURE 6. (a) Power deposition on diagnostic calorimeter, Pulse #6308 (Hydrogen, RF power of 2 x 62 kW, U_{HV} = 30 kV, I_{PG} = 2 kA, I_{bias} = 55 A, j_{extr} =12.3 mA/cm^2, j_e/j_{extr} = 0.5), divergence 1.17°, (b) corresponding eight gaussian fit.

Beamlet divergence evaluation

In order to validate the fitting procedure, a comparison of the data obtained from the IR thermography with the Beam Emission Spectroscopy diagnostic (BES) has been performed. At first only beam pulses in which one of the two generators was used have been considered, i.e. the plasma was generated either in the two upper or the two lower drivers only. This mode of operation leads to the production of roughly only "half" of the negative ion beam, so only superposition in the horizontal direction occurs for the corresponding beamlet groups. An example of the beamlet group widths (σ_x horizontal and σ_y vertical directions) and of their correlations with the divergence as estimated by BES (vertical line of sight located at the beamlet group #2 and #6, LoS#19) is displayed in FIGURE 7(a). The beamlet optical quality can be described by means of the perveance Π, which is defined by:

$$\Pi = \frac{I_{ex}}{U_{ex}^{\frac{3}{2}}}, \qquad (1)$$

where I_{ex} is the extracted total current and U_{ex} is the extraction voltage.

A dependence of beamlet group widths from the normalized perveance (for the same beam pulses) was observed, as expected. In FIGURE 7(b) it is shown how the beamlet group widths follow the typical parabolic pattern of the divergence versus normalized perveance. A good correlation between the beamlet group widths and the divergence measured by BES, together with their correlation with perveance, suggest that the widths obtained by the fit of the power density profile could be strictly linked to the beamlet divergence. However, in order to find the relation between the beamlet divergence and the widths of the beamlet groups as obtained by the fit of the power beam deposited on the diagnostic calorimeter, some simulations have been performed.

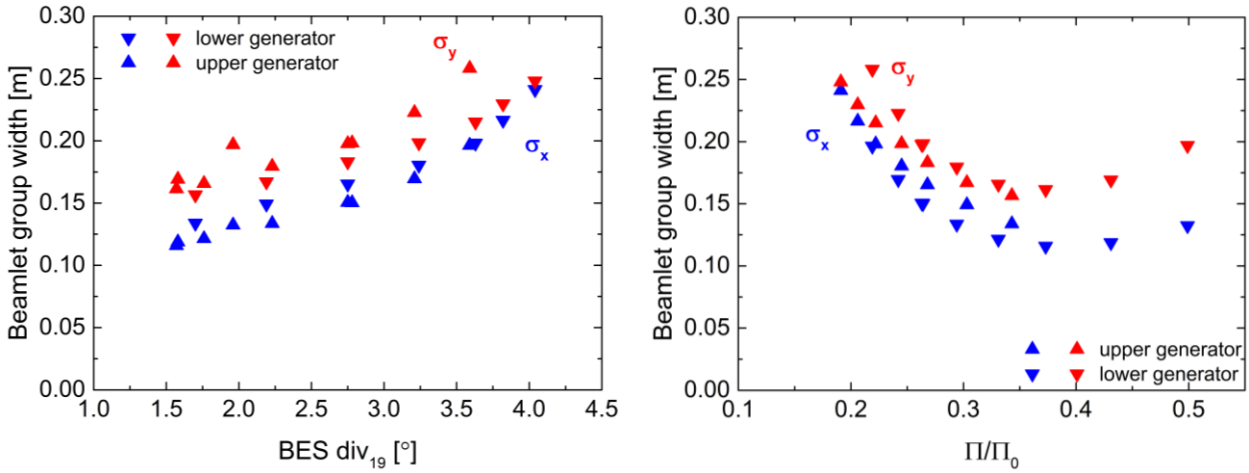

FIGURE 7. (a) Beamlet group width versus divergence measured by BES on LoS #19. (b): beamlet group widths versus normalized perveance.

The beam power was simulated as the superposition of 640 gaussians (i.e. gaussian distribution of the current density), one for each beamlet, using the geometry of the grids of ELISE (no focusing effect is present, because the grids are planar and the apertures are aligned). No information about the source processes or the beam optics is included; no deflections due to magnetic or electric filter fields are considered. The divergence and the amplitude of each current beamlet has been defined as input and propagated geometrically to 3.5 m distance, where their overlapping generates the 2D power distribution map as observed on the calorimeter. As a first step, a completely homogeneous beam has been taken into account: for a given amplitude of all the 640 gaussian functions, the beamlet divergence has been varied, but kept equal between all the 640 beamlets. The fitting procedure described in the previous paragraph has been applied to these simulations, so that a relation between the beamlet divergence and the gaussian widths was found. This relation is displayed in FIGURE 8.

Since the beamlet group has an intrinsic width, given by the position of the apertures in the extraction grids, a sort of "saturation" of the value of the gaussian widths for lower beam divergence is expected. This kind of saturation was seen for σ_y, corresponding to about 10 cm. This value correspond to a half 1/e width of 14 cm, which compared to the initial beamlet group half width of 16 cm (8 beamlet x 20 mm in diameter) is a reasonable result. The saturation of the horizontal width is expected to occur at a value in the order of σ_x = 3.5 cm since the initial half width of the beamlet group in the horizontal direction is about 5 cm. This saturation is out of the simulations displayed in FIGURE 8. These curves have been used to obtain the beamlet divergence from the gaussian widths calculated from fitting the IR data on the beam power deposition from the diagnostic calorimeter, under the assumption of a fully homogeneous beam. The beamlet divergence evaluated in this way has been compared with the divergence

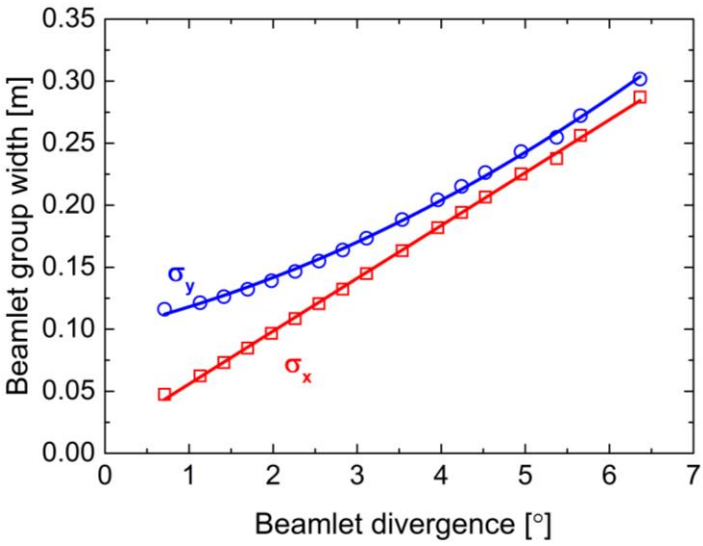

FIGURE 8. Relation between beamlet divergence used as input in an ELISE beam simulation and gaussian widths of the beamlet groups obtained from a gaussian fit of the resulting beam power distribution on the calorimeter, placed at 3.5 m from the grounded grids of ELISE. σ_x is the horizontal width, while σ_y is the vertical width.

estimated by BES. The divergence evaluated via IR thermography results to be larger than the BES estimate by 20-30%. This disagreement is under investigation [16].

Beam inhomogeneity: macroscopic and local features

In ELISE, even for the lowest divergences achieved (1°, in D operation), the beamlets are not distinguishable at 3.5 m distance from the grounded grid, where the calorimeter is placed. The definition of inhomogeneity is therefore based on the relative intensity of the eight beamlet groups. The total power associated to each beamlet group was be evaluated by the volume of a 2D gaussians for each beamlet group obtained from the gaussian fit.

For short pulses at low power (10 s HV-phase in a 20 s RF pulse; RF power up to 80 kW, U_{HV} up to 35 kV), a low beam inhomogeneity is found. The contributions from the four beamlet group on the left side of the calorimeter (panels 1 and 3) are of the same order of the ones on the right side (panels 2 and 4); the inhomogeneity seems to be slightly smaller in D (1%) than in H (up to 5%). In Deuterium, also a low top-bottom inhomogeneity is found between the upper and lower rows of beamlet groups; for Hydrogen a large inhomogeneity (up to 30%) seems to be present (the power on the beamlet groups bottom row is higher than on the upper row), but this is probably related to the conditioning phases of the source operation. Work on this topic is still ongoing.

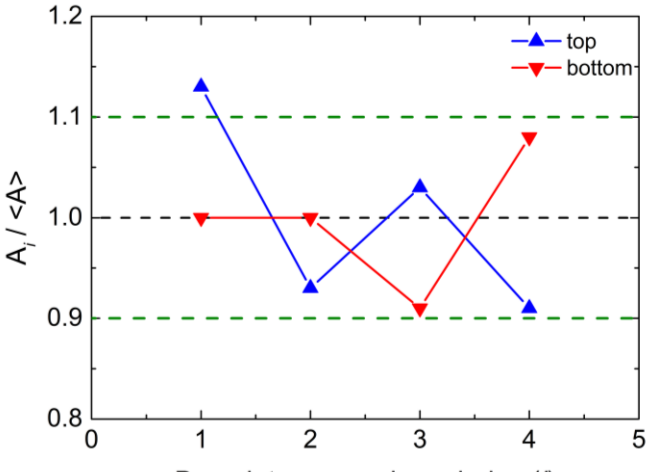

FIGURE 9. Example of a typical ratio between the eight fitting gaussian amplitudes and their average along a single row for pulses in H. Blue squares are for the upper row, red ones for the lower one. The green horizontal dashed lines represent the ITER limits for beam inhomogeneity.

On a local scale, some considerations about each beamlet group can be carried out. Since all the beamlet groups of the upper and lower row, respectively, are fitted using the same widths, the inhomogeneity within a beamlet group row is described by the ratio of the gaussian amplitudes A_i (i from 1 to 4 for the upper row; from 5 to 8 for the lower one) to the row average amplitudes, $\langle A \rangle_{top}$ or $\langle A \rangle_{bottom}$. All the data are well fitted by straight lines and the statistical error given by the fit on the angular coefficients is very low (0.01). Using the slopes of the fitting lines as an average amplitude ratio to apply the definition of inhomogeneity to the beamlet groups, a maximum inhomogeneity of 13% for the upper group line and 9% for the lower row are obtained in H. These considerations are valid also for D operation, but with slightly smaller differences (inhomogeneity only up to 11% for the upper row; 6% for the lower one). The ratio between the eight beamlet group amplitudes A_i and the total average values <A> (here each A_i is the average of the amplitudes for each beamlet group for all the hydrogen pulses analyzed so far), is displayed in FIGURE 9.

The profile is not flat and does not show any particular trend (for example larger amplitudes in the center or at the borders) but the amplitudes have some fluctuations from group to group. A sensitivity analysis of the fit with respect to reproducing profiles with such amplitude patterns has been successfully completed, therefore a failure of the fit procedure is excluded. It has been observed that this inhomogeneity seems to decrease (in percentage) for lower divergence. At the moment, this topic is still under investigation.

SUMMARY AND CONCLUSIONS

The large negative ion source testbed ELISE has been equipped with several beam diagnostic tools in order to evaluate beam characteristics, in particular divergence and inhomogeneity. The most sophisticated beam diagnostic tool in ELISE is the diagnostic calorimeter, which has been installed in ELISE at the end of 2013. The calorimeter is equipped with 48 thermocouples to measure beam power profiles, sensors for water calorimetry and is accompanied by a high-resolution thermo-graphic camera that allows a 2D reconstruction of the beam power/ion-current distribution. The copper calorimeter has been coated with an IR black coating to increase the surface emissivity. The

thermocouples embedded in the calorimeter and the thermo-graphic camera allow to estimate the coating emissivity coefficient in the IR range, which is essential to calibrate the thermography diagnostic. Total beam power/ion currents obtained by water calorimetry and IR thermography agree within 10% of uncertainty.

From the analysis of the IR thermography data, based on fitting the power density matrix with 8 gaussian sub-beams, one for each beamlet group, beam divergence and inhomogeneity are obtained. This procedure has been benchmarked using a simulation of the beam represented by the superposition of 640 gaussian beamlets (as much as extracted in ELISE) of given equal divergence as a reference. The beam divergence measured by IR thermography is in the range 1° to 4° and results 20-30% larger than the one obtained from beam emission spectroscopy.

Beam inhomogeneity has been measured by means of gaussian fit in terms of difference between the intensities of the beamlet groups. The average beam inhomogeneity was found to be below 13% and tends to decrease for lower beam divergence.

ACKNOWLEDGMENTS

The work was supported by a contract from Fusion for Energy (F4E-2009-0PE-32-01), represented by Antonio Masiello, with an amount of 4 M€. The opinions expressed herein are those of the authors only and do not represent the official positions of Fusion for Energy and of the ITER Organization.

REFERENCES

[1] Hemsworth, R. et al., "Status of the ITER heating neutral beam system", Nuclear Fusion, v49, 045006, (2009).
[2] Schunke, B. et al., "Status of the negative ion based Diagnostic Neutral Beam for ITER," Proceedings of the 24th IAEA Fusion Energy Conference. (2012) p. ITR/P1-03.
[3] E. Speth, et al., "Overview of the RF source development programme at IPP Garching," Nucl. fusion 46 (2006) 220.
[4] Stäbler et al. "Development of a RF-driven ion source for the ITER NBI system," Fus. Eng. Des. 84, 265-268 (2009).
[5] W. Kraus, et al., "The development of the radio frequency driven negative ion source for neutral beam injectors," Review of Scientific Instruments 83 (2012) 02B104.
[6] P. Franzen, et al., "Progress of the development of the IPP RF negative ion source for the ITER neutral beam system," Nucl. Fusion 47 (2007) 264.
[7] U. Fantz, et al., "Physical performance analysis and progress of the development of the negative ion RF source for the ITER NBI system," Nucl. Fusion 49 (2009) 125007.
[8] B. Heinemann, et al., "Design of the “half-size” ITER neutral beam source for the test facility ELISE,” Fusion Eng. Des. 84 (2009) 915.
[9] B. Heinemann, et al., "The negative ion source test facility ELISE," Fusion Eng. Des. 86 (2011) 768.
[10] Franzen P. et al., "Status of the ELISE test Facility," this conference.
[11] R. Nocentini, et al., "Towards a large RF ion source for the ITER neutral beam injector: Project overview and first results of ELISE," IEEE Transactions on Plasma Science, Vol. 42, No.3, (2014).
[12] U. Fantz, et al., “Size scaling of negative hydrogen ion sources for fusion,” this conference.
[13] M. Fröschle, et al., “Magnetic filter field for ELISE – Concepts and Design,” Fusion Eng. Des. 88 (2013) 1015-1019.
[14] D. Wünderlich, et al., "Optical emission spectroscopy at the large RF driven negative ion test facility ELISE: Instrumental setup and first results," Rev. Sci. Instrum., vol 84, no. 9, pp. 093102-1-093102-6 (2013).
[15] R. Nocentini, et al., "Beam Diagnostic Tools for the negative hydrogen ion source test facility ELISE," Fus. Eng. Des. 88, 913-917 (2013).
[16] F. Bonomo, et al., "BATMAN Beam Properties Characterization by the Beam Emission Spectroscopy Diagnostic," this conference.